



Swansea University
Prifysgol Abertawe



Cronfa - Swansea University Open Access Repository

This is an author produced version of a paper published in :

Cronfa URL for this paper:

<http://cronfa.swan.ac.uk/Record/cronfa7038>

Book chapter :

Belblidia, F., Haroon, T. & Webster, M. (2009). *The Dynamics of Compressible Herschel—Bulkley Fluids in Die-Swell Flows*.(pp. 425-434).

http://dx.doi.org/10.1007/978-90-481-2669-9_45

This article is brought to you by Swansea University. Any person downloading material is agreeing to abide by the terms of the repository licence. Authors are personally responsible for adhering to publisher restrictions or conditions. When uploading content they are required to comply with their publisher agreement and the SHERPA RoMEO database to judge whether or not it is copyright safe to add this version of the paper to this repository.

<http://www.swansea.ac.uk/iss/researchsupport/cronfa-support/>

The Dynamics of Compressible Herschel–Bulkley Fluids in Die-Swell Flows

Elblidia¹, T. Haroon² and M.F. Webster¹

¹Institute of non-Newtonian Fluid Mechanics, School of Engineering, Swansea University, Singleton Park, Swansea, SA2 8PP, UK

²Visiting researcher, COMSATS Institute of Information Technology, Abbottabad, Pakistan

Abstract In a variety of industrial applications, modelling compressible inelastic free-surface flows remains a numerical challenge. This is largely due to the physical phenomena involved and the computational cost associated with the simulations of such flows. In particular, the die-swell problem is characterised by specific features. These are related to the presence of a flow separation point at the die-exit, the location and the shape of the free-surface, and finally the consideration of fluid compressibility under various forms of material modelling. In this article, a time-marching pressure-correction scheme is considered to solve both incompressible and compressible inelastic flows. This is achieved via a pressure-based approach within a finite element framework employing efficient high-order time-stepping schemes. A constitutive model is utilised to express the equation of state that links density to pressure, so that pressure is retained as a primary variable. Various material models are considered in this numerical study for the die-swell problem, where the material rheological characteristics have a significant impact upon the location and form of the free-surface. Initially, unyielded material is modelled through Newtonian and power-law assumptions. Further complication is then introduced through the Bingham model, where fluid yield stress is taken into account. More complex rheological modelling is constructed via the Herschel–Bulkley model, combining viscoplastic behaviour with yield stress presence. This is complimented by relaxing incompressibility assumptions, allowing the effects of compressibility to enter the problem. Results are presented for steady and transient flow scenarios and numerical solutions are validated against published data. Here is Focus upon on the effect of variation in compressibility parameter setting, inertia parameter, power-law index and yield stress level, with regard to the evolving shape/location of the free-surface and the response in extrudate swell. Extrudate swell is observed to decline with increase in power-law index. With increase in Reynolds number, extrudate swell decreases initially, finally reaching a plateau at high Reynolds number, in agreement with experimental observations. Swelling also decreases with rise in yield stress levels. The combination of these features within the compressible Herschel–Bulkley model renders it difficult to predict, a significant challenge in the outcome in terms of die-swell behaviour.

Keywords: Die-Swell, Inelastic, Power-Law, Bingham, Herschel–Bulkley Model, Yield Stress.

1 Introduction

Over the past decades, extruded materials include metals, ceramics, polymers, paints, coatings and composites. Much research has focused attention on low pressure, high flow

ion processes in an effort to better understand and prevent interfacial instabilities. The die-swell problem naturally introduces free surface modelling, unsteady transient evolution states, material rheology and influence of compressibility. In spite of a variety of industrial applications, modelling compressible surface flows itself remains a numerical challenge, largely due to the physical phenomena involved. For example, the *free surface* of the jet introduces mixed-boundary conditions on the flow. Various slip (velocity) conditions may be present on the tube wall, while the jet itself supports traction (or stress) boundary conditions. This local and sudden change in the type of boundary conditions will create a singular stress field, accompanied with steep velocity gradients. There are many approaches to treat free surface computations, such as the volume of fluid technique (VOF), marker and cell method (MAC) and the arbitrary Lagrangian-Eulerian (ALE) scheme. Most studies have assumed incompressible flow and modelled material through Newtonian or power-law model. A yield stress response can be adapted through the Bingham model, or with inelastic effects, through the viscoelastic-Bulkley model. To date, the extrusion problem has attracted much interest in the literature. Beverly and Tanner [1] analysed the effects of yield stress on die swell in a tube, and found that yield stress inclusion reduced the degree of swell. Mitsoulis and co-workers [2] studied entry and exit flows of Bingham fluid, observing the presence of unyielded regions within the flow. Compressible viscoelastic domain remains relatively uncharted in the literature, Georgiou [3] addressed non-Newtonian inelastic fluid modelling for compressible flows, showing interest in slip effects. In addition, compressible flow computations are covered by Webster and co-workers [4, 5].

Governing equations

For an incompressible Newtonian fluid flow under isothermal setting, the governing equations may be expressed in non-dimensional form as:

$$\frac{\partial \rho}{\partial t} + \nabla \cdot (\rho \mathbf{u}) = 0 \quad (1)$$

$$\text{Re} \frac{\partial \mathbf{u}}{\partial t} = \nabla \cdot \boldsymbol{\tau} - \text{Re} \mathbf{u} \cdot \nabla \mathbf{u} - \nabla p \quad (2)$$

where the field variables are ρ , \mathbf{u} , $\boldsymbol{\tau}$, p , for density, velocity, stress and pressure, respectively. $\text{Re} = \rho_0 U \cdot l / \mu_0$ represents the conventional dimensionless Reynolds number.

The stress is related to field kinematics through a constitutive law, which is defined

$$\tau_{ij} = \mu(d_{ij} - 2/3(\nabla \cdot u)\delta_{ij}) \quad (3)$$

μ is the viscosity (constant or function of shear-rate, see on), δ_{ij} is the Kronecker tensor, $2d = \nabla u + \nabla u^T$ is the rate of deformation tensor, and the $2/3$ vanishes under incompressible assumptions. Further equations are necessary (below), relating to free surface computation, material modelling and compressibility considerations.

Compressibility considerations

For compressible flow settings, the modified two-parameter (B, m) Tait equation is considered to relate density to pressure. Thus,

$$(p + B)/B = \rho^m \quad (4)$$

Differentiating the equation of state, one gathers [4]:

$$\frac{\partial p}{\partial \rho} = \frac{m \cdot (p + B)}{\rho} = c_{(x,t)}^2 \quad (5)$$

where $c_{(x,t)}$ is the derived speed of sound. Such dependencies have influence upon the free surface evolution.

Free surface considerations

For the extrusion flow problem, no-slip boundary conditions are assumed along the die walls, and free kinematic conditions on the free surface. This generates a singular velocity field at the die-exit. On the free surface, zero normal velocity, zero shear stress and normal stress are set. We appeal to the evolving free surface equation:

$$\frac{\partial h}{\partial t} = u_r - v_z \frac{\partial h}{\partial z} \quad (6)$$

where $u = (u_r, v_z) = (\partial r / \partial t, \partial z / \partial t)$ is the velocity vector and $h = h(x, t)$ is the radial coordinate. The die-swell ratio is defined as $\chi = h_f / h_0$, where h_f and h_0 are the final extrudate radius and die radius, respectively (see Fig. 1).

The ALE-technique is performed to radially adjust mesh.

Material modelling considerations

so-called ‘yield stress τ_0 ’ (first introduced by [7]), governs the transition from solid-like to liquid-like response. It is the presence of yielded and unyielded regions across the domain, which provides the intrinsic discontinuity within the flow. To overcome this deficiency, several modifications have been proposed (see [8] for a review). The power-law model allows for a degree of deviation from Newtonian behaviour ($n = 1$). Thus, shear-thinning is observed for $n < 1$, and $n > 1$ corresponds to shear-thickening. The generalised Herschel–Bulkley (HB) model provides further physical richness, incorporating both power-law type and Bingham type.

Flow equations

For non-Newtonian fluids, the viscosity is considered as a nonlinear function of the second invariant (Π_d) of the rate-of-strain tensor (d_{ij}), which modifies (3) accordingly. A Bingham material remains rigid when the shear-stress is below the yield stress τ_0 , but flows like a Newtonian fluid when the shear-stress exceeds τ_0 :

$$\tau = \begin{cases} \mu + \frac{\tau_0}{2|\Pi_d|^{\frac{1}{2}}} \cdot \dot{\gamma} & \text{for } |\Pi_\tau| > \tau_0^2; \text{ and } \dot{\gamma} = 0 \text{ for } |\Pi_\tau| \leq \tau_0^2 \end{cases} \quad (7)$$

Papanastasiou [8] proposed a modified Bingham model, by introducing a regularisation stress growth exponent (m) to control the rate-of-rise in stress, in the

$$\tau = \begin{cases} \mu + \tau_0 \frac{1 - e^{-m|\Pi_d|}}{2|\Pi_d|^{\frac{1}{2}}} \end{cases} \cdot \dot{\gamma} \quad (8)$$

Other rheological derivations to accommodate for shear characteristics, may be considered through power-law model:

$$\tau = \left(k \cdot |\dot{\gamma}|^{n-1} \right) \cdot \dot{\gamma} \quad (9)$$

where k is the consistency parameter.

As the Herschel–Bulkley (HB) model that incorporates both a yield stress and shear behaviour. To address the shortcoming of infinite apparent viscosity at vanishing shear-rates Mitsoulis [9] Alexandrou et al. [10] introduced the modified

$$= \begin{cases} k \frac{n-1}{\Pi_d^2} + \tau_0 \frac{1 - e^{-m|\Pi_d|}}{|\Pi_d|^{\frac{1}{2}}} & \text{for } |\Pi_\tau| > \tau_0^2; \text{ and } \dot{\gamma} = 0 \text{ for } |\Pi_\tau| \leq \tau_0^2 \end{cases} \quad (10)$$

Numerical discretisation

The fractional-staged Taylor–Galerkin incremental pressure-correction (TGPC) work is considered (see [4, 5] for derivation). The *first phase* involves a predictor–corrector doublet (Lax–Wendroff) for velocity and stress. The *second phase* is a pressure-correction scheme that ensures second-order accuracy in time. The *third phase* recaptures the velocity field at the end-of-time step loop. Triangular element is employed based on a quadratic velocity and linear pressure approximations. For density, a piecewise-constant interpolation is employed, with averaged density gradients, over an element. The discrete compressible TGPC can be expressed via Eqs. (11–14). Note, the equations for compressible and incompressible flows differences appear mainly under the continuity equation (13).

Stage 1a :

$$\frac{M_\rho}{\Delta t/2} + \frac{1}{2} S_u \left[\left(\Delta U^{n+\frac{1}{2}} \right) \right] = - \left[S_u U + N_\rho(U) U - L^T \left\{ P^n + \theta_1 (P^n - P^{n-1}) \right\} \right] P^n \quad (11)$$

Stage 1b :

$$\frac{M_\rho}{\Delta t} + \frac{1}{2} S_u \left[\left(\Delta U^* \right) \right] = - \left[S_u U - L^T \left\{ P^n + \theta_1 (P^n - P^{n-1}) \right\} \right] P^n - \left[N_\rho(U) U \right]^{n+\frac{1}{2}} \quad (12)$$

Stage 2 :

$$\left[\frac{M_C}{\Delta t^2} + \theta \cdot K \right] \left(\Delta P^{n+1} \right) = - \frac{1}{\Delta t} L_P \cdot U^* \quad (13)$$

Stage 3 :

$$\frac{M_\rho}{\Delta t} \left(U^{n+1} - U^* \right) = \theta L^T \left(P^{n+1} - P^n \right) \quad (14)$$

Numerical results and discussion

approach is to start by analysing an incompressible Newtonian fluid and then systematically introduce further complexity through inertia, compressibility, generalised Newtonian and HB representation. The capillary radius is held constant ($R = 1$) and only half of the die-swell domain is analysed (symmetry). Applied boundary conditions and die-swell dimensions are supplied in Fig. 1.

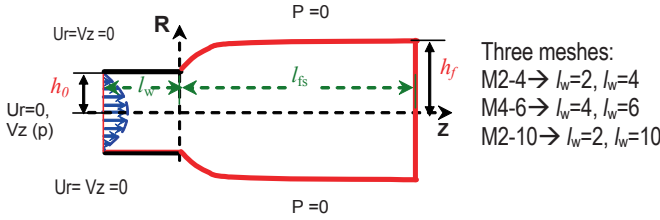


Fig. 1. Die-swell schema

Newtonian case

Effect of die-swell design and mesh consistency analysis

Effects of mesh refinement, extrudate length and capillary length on the swelling are analysed. During the transient development, one observes a common minimum swelling at the same location followed by different swelling ratio steps. The jet, being larger with longer jet-lengths.

Once a steady development is achieved, swelling height reaches the ratio of 1.5, independent of the level of refinement used. The transient pressure response is observed instantaneously, following a linear development trend in pressure-drop.

Effect of inertia

A generally accepted finding is that under incompressible assumptions, the jet swelling reduces as inertia (Re) increases, see Georgiou and co-workers [11]. This is clearly illustrated in Fig. 2, when based on mesh M2-4, we detect two distinct regimes: below $Re = 7.5$, there is expansion through jet swelling, whilst, above this level, we observe compression of the jet, reaching a plateau of $\chi = 0.91$ at levels of $Re > 40$. There is a clear evidence of pressure-drop reduction as Re increases.

Influence of compressibility

Newtonian fluids and various compressible settings ($Ma = 0.0$ to $Ma_{\max} = 0.55$), the free surface shape and extrudate swell-ratio are insignificantly affected by the proposed die-swell designs and mesh refinements. This fact was also highlighted by Georgiou [12]. This is mainly due to the imposition of no-slip boundary conditions on the wall. Detailed analysis of various slip conditions is the subject of future study.

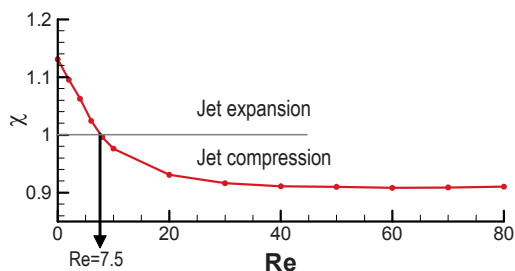


Fig. 2. Inertial effect on jet swelling; incompressible, Newtonian

Elastic power-law representation

Effect of power-index (n)

Variation of swelling ratio with power-index is depicted in Fig. 3. , under $Ma = 0$. Here, a longer channel length (M4-6) is selected to allow for the full development of the velocity profile from its parabolic inlet state. In agreement with Mitsoulis [13] findings, the general trend is that die-swell increases with the use of power-law index n , except in the range $0 < n < 0.2$, where a slight contraction or negative swell is observed.

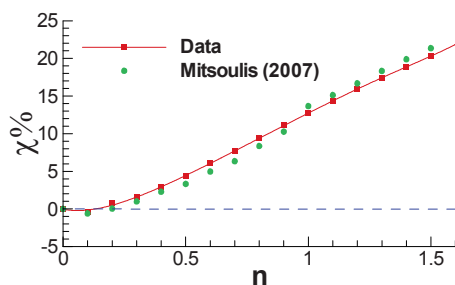


Fig. 3. Die-swell as a function of power-law index n for the power-law model

Viscoplasticity-Bingham yield stress

analyse the effect of yield stress on the flow based on the modified Bingham model. The (χ)-response against Bn is shown in Fig. 4.

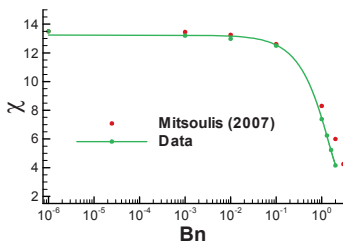
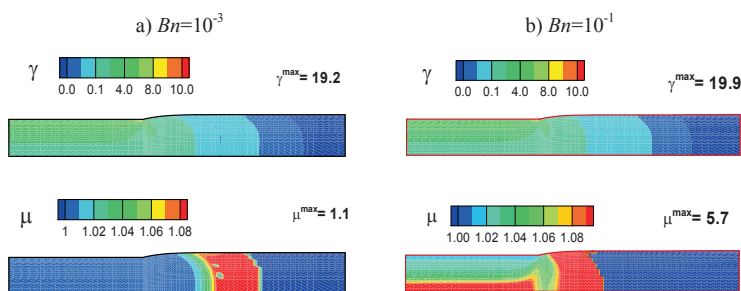


Fig. 4. Swelling ratio as function of yield stress with modified Bingham model

we observe a substantial decrease of swelling for levels of yield stress above 0.01, whilst there is a sustained plateau in swelling for Bn below 0.01, as in [13]. Early, the pressure-drop increase with increased yield stress, as the increase is more pronounced for $Bn > 0.1$, whilst, pressure remains relatively constant over the Bn -range.

Herschel–Bulkley modelling

Flowing under the HB-model is governed by the variation of both power-law index n and yield stress τ_0 . At steady-state, the swelling under $n = 0.9$ and $\tau_0 = 0.1$ reaches a level of $\chi = 1.1$, as already observed under power-law modelling (Fig. 4). This position is not affected by the yield stress level over this plateau range of Bn (see Fig. 4). Steady-state shear-rate and viscosity contour plots for $n=0.9$ at two levels of $Bn=10^{-3}$ and 10^{-1} are depicted in Fig. 5. The shear-rate contours are similar for both levels of yield stress, whilst there is a clear increase in the maximum viscosity attained at larger τ_0 applied.



Conclusions

Die-swell benchmark problem naturally introduces free surface modelling, separation point at the die-exit, provocative transient evolution states and initial modelling. Focus is placed on the jet shape dynamic evolution and the surface location. Steady and transient flow situations are presented under incompressible and compressible assumptions, with findings validated against published data. Initially, unyielded material is considered through Newtonian and power-law assumptions. Further complication is then introduced through the Bingham model, where fluid yield stress is taken into account. Subsequently, a rheological generalisation is built via the Herschel–Bulkley model.

The study demonstrated that extrudate swell is unaltered by compressibility considerations under no-slip wall conditions. However, it is expected that this position will be altered under slip-wall settings. The swelling is observed to decline with increase in power-law index. Swelling also decreases with rise in yield stress. Therefore, predictions remain difficult, a priori, under the parameters variation within the Herschel–Bulkley model. Further challenges posed will be met from its generalised Herschel–Bulkley model, to a novel visco-elasto-plastic material modelling, permitting a direct comparison across regimes for compressible representation, ranging from viscoplastic, to viscoelastic, to visco-elasto-plastic alternatives.

Acknowledgments We gratefully acknowledge financial support under the EPSRC grant ‘Complex Fluids and Complex Flows – Portfolio Partnership’, TH acknowledge research visit funding from HEC of Pakistan.

References

- B.R. Beverly and R.I. Tanner. Numerical Analysis of Extrudate Swell in Viscoelastic Materials with Yield Stress. *J. Rheol.* 33 (1989) 989–1009.
- S. Abdali, E. Mitsoulis and N.C. Markatos. Entry and exit flows of Bingham fluids. *J. Rheol.* 36 (1992) 389–407.
- C. Georgiou. The time-dependent, compressible Poiseuille and extrudate-swell flows of a Carreau fluid with slip at the wall. *J. Non-Newt. Fluid Mech.* 109 (2003) 93–114.
- M.F. Webster, I.J. Keshtiban and F. Belblidia. Computation of weakly-compressible highly-viscous liquid flows. *Eng. Comput.* 21 (2004) 777–804.
- I.J. Keshtiban, F. Belblidia and M.F. Webster. Numerical simulation of compressible viscoelastic liquids. *J. Non-Newt. Fluid Mech.* 122 (2004) 131–146.
- G. Tait, Physics and Chemistry of the Voyage of H.M.S. Challenger, 2, Part IV (1888), HMSO, London, England.
- R.C. Bingham. Fluidity and Plasticity. McGraw-Hill, New York, 1922.
- C. Papanastasiou. Flows of materials with yield. *J. Rheol.* 31 (1987) 385–404.
- E. Mitsoulis. Numerical simulation of planar entry flow for a polyisobutylene solution using an integral constitutive equation. *J. Rheol.* 37 (1993) 1029–1040.
- N. Alexandrou, T.M. McGilvray and G. Burgos. Steady Herschel–Bulkley fluid flow in

F. Belblidia et al.

- Taliadorou, G.C. Georgiou and E. Mitsoulis. Numerical simulation of the extrusion of strongly compressible Newtonian liquids. *Rheol. Acta* 47 (2008).
- G.C. Georgiou. The compressible Newtonian extrudate swell problem. *Int. J. Num. Meth. Fluids* 20 (1995) 255–261.
- E. Mitsoulis. Annular extrudate swell of pseudoplastic and viscoplastic fluids. *J. Non-Newt. Fluid Mech.* 141 (2007) 138–147.